ELSEVIER

Journal of Power Sources 101 (2001) 1–9

JOURNAL OF POWER SOURCES

www.elsevier.com/locate/jpowsour

Influence of carbon black and binder on Li-ion batteries

L. Fransson*, T. Eriksson, K. Edström, T. Gustafsson, J.O. Thomas

Materials Chemistry, Ångström Laboratory, Uppsala University, P.O. Box 538, SE-751 21 Uppsala, Sweden

Received 18 September 2000; received in revised form 21 December 2000; accepted 30 December 2000

Abstract

The electrochemical response of different components such as carbon black (CB), binder, current collector and lithium salt have been examined in a general Li-ion battery context. The influence of these various components, alone and in different combinations, on composite graphite anodes and $LiMn_2O_4$ cathodes was addressed. CB electrodes were found to cycle with a reversible capacity of 180 mAh/g between 0.01 and 1.5 V, but with an irreversible capacity of 70%. The effect of adding CB to graphite electrodes was quantified in terms of first-cycle irreversible capacity and reversible capacity. Cyclic voltammetry measurements on CB electrodes were made in the same voltage region using different binders and electrolyte salts. A clear difference could be discerned between using EPDM or PVdF binder; extra reduction reactions were observed for the PVdF binder at 0.35 V. The thermal behaviour of these binders in CB electrodes was also examined in the temperature range 30–300°C. The role of the anion in terms of thermal stability was also quantified from DSC measurements on both CB and graphite electrodes; the starting temperature for exothermal reactions involving SEI-layer reactions is clearly lower (∼60°C) for $LiBF_4$ than $LiPF_6$ (∼110°C) for both CB and graphite electrodes. Cyclic voltammetry in the cathodic region (3.0–5.5 V) showed oxidation reactions between non-fluorinated binders, CB and $LiPF_6$. These reactions could be avoided by changing to $LiBF_4$. The electrochemical response on using fluorinated and non-fluorinated binders in this voltage region showed clear differences.

Keywords: Carbon black; Binder; Electrolyte decomposition; Thermal stability

1. Introduction

Li-ion batteries have been studied in detail, by many research groups over the past years. The ''rocking-chair'' concept with, for example, graphite as anode and $LiMn_2O_4$ as cathode is one example [1–3]. In most of these Li-ion concepts, carbon black (CB) has been used to improve electrical conductivity between the active particles. A binder is also added to help counter volumetric changes occurring in the insertion electrodes during intercalation/deintercalation and to ensure adhesion to the current collectors.

There have been several reports on CB as a potential anode material in the Li-ion battery [4–8], but it has been found to give a relatively low charge/discharge capacity and a large first-cycle irreversible capacity. Given the high surface area compared to other carbon materials, electrolyte reduction on the CB is likely to contribute substantially to the first-cycle irreversible capacity through the formation of a solid electrolyte interphase (SEI)-layer. It is, therefore, important to probe what effect adding CB to negative electrodes has on first-cycle irreversible capacity. Several authors have also studied the temperature stability of carbonaceous anodes [9–11]. Temperature stability is an important safety issue, typically in portable applications.

Adding CB to the composite cathode has also proven to increase cycle life and decrease polarisation of the electrode [12]. High surface area CB is also relevant to the electrolyte reactions occurring at the cathode. In the case of $LiMn_2O_4$ cathodes, an irreversible capacity, having its origin in oxidation reactions, was found to depend strongly on the CB content in the electrode [13]. Manganese dissolution from $LiMn_2O_4$ as result of the carbon additive was found to increase for larger surface-area carbon, while polarisation of the cell is greater for smaller surface-area carbon [14].

To optimise the Li-ion batteries, it is essential to study all the electrode components individually, and not only the high-performance electrode materials as such. We have studied the effects CB and type of binder have on Li-ion cell performance under normal conditions, and at elevated temperatures, both in the low-potential and high-potential region. The temperature stability of the SEI-layer formed on CB is compared to that formed on a composite graphite

* Corresponding author. Tel.: +46-18-471-3735; fax: +46-18-51-3548.
E-mail address: linda.fransson@angstrom.uu.se (L. Fransson).

0378-7753/01/$ – see front matter
PII: S0378-7753(01)00481-5

anode. This is done for electrolytes with two different salts ($LiBF_4$ and $LiPF_6$) using different types of binder. We have chosen to compare a commonly used fluorinated binder (PVdF) with two non-fluorinated binders (EPDM and Kraton G), since fluorinated hydrocarbons are known to constitute an environmental risk; well-known examples are the ozone depletion compounds. Fluorinated hydrocarbons are persistent and foreign to nature; from an environmental point of view it is, therefore, interesting to investigate alternatives. One development in today's Li-ion batteries is towards cathode materials operating in the 5 V region [15]. We, therefore, extend the potential-window to 5.5 V, to gain information about the electrochemical properties of the binder and the commonly used graphitised aluminium current collector in combination with electrolytes containing different salts.

2. Experimental

2.1. Half-cell preparation

The CB powder (Shewinigan Black), natural graphite powder from the Woxna mine, Tricorona AB, Sweden or synthetic graphite (Timrex KS6, Timcal A + G Sins, Switzerland) and $LiMn_2O_4$ (Selectipur®, Merck, Darmstadt, Germany) were used in the electrode fabrication. BET measurements were made using a Flow Sorb 2300 (30 vol.% N_2/He) to determine the surface area of the powders. The surface area was measured on the original powders as well as on powders that had been ball-milled in cyclohexane. XRD measurements were also performed on the original CB powder using a Siemens D5000 diffractometer. The mosaic-block size was determined using Scherrer's formula.

Graphite anodes were prepared with three different compositions: 10:80:10, 30:60:10 and 50:40:10 wt.% of CB/graphite/EPDM, respectively. $LiMn_2O_4$-based cathodes were made with a composition 15:80:5 wt.% CB/$LiMn_2O_4$/EPDM. Electrodes were also prepared from 90 wt.% CB and 10 wt.% binder. Ball-milling was used in making the CB electrodes, where the three different binders used were: EPDM (ethylene propylene diene terpolymer) in cyclohexane, PVdF (polyvinylidene fluoride) in NMP (1-methyl-2-pyrrolidinone), and Kraton G (a starblock-copolymer with polyisopropene and poly((ethene-co-buten)-block-styrene)) in cyclohexane. All slurries were ball-milled for 20 min and then extruded onto a Cu- or Al-foil, depending on whether it was to be used in the low- or high-potential region. Both graphitised and untreated Al-foils were used. Electrode discs of area 3.14 cm^2 were cut out and dried in a vacuum furnace at 120°C for 4 h prior to use.

Two- and three-electrode coffee-bag cells were manufactured in an argon-filled glove-box (<2 ppm O_2 and H_2O), using the CB containing electrodes as working electrode and lithium as counter electrode, separated by glass fibre soaked in electrolyte. In the case of three-electrode cells, lithium was used as reference electrode together with an extra glass fibre separator. The electrolytes used were a 1 M solution of $LiBF_4$ (Tomiyama) or 1 M $LiPF_6$ (Merck) in EC/DMC 2:1 by volume (Selectipur®, Merck, Darmstadt, Germany). The $LiPF_6$ and $LiBF_4$ salts were dried in a vacuum furnace at 80 and 120°C, respectively, for 12 h prior to use. The glass fibre was dried at 140°C in the same way. The electrolytes had a water content of <20 ppm, determined by Carl Fischer titration.

2.2. Low-potential region

The 0.01–1.5 V versus Li/Li^+ range is hereafter referred to as the low-potential region. For capacity measurements, galvanostatic mode was used on a Digatron BTS-600 with a constant current density of around 0.03 mA/cm^2, which gives about C/12. Cyclic voltammetry was also performed using a Radiometer Copenhagen PGP201, with a scan rate of 10 mV/min. The cyclic voltammetry measurements were performed on CB electrodes with two different binders (EPDM or PVdF) in electrolytes containing $LiBF_4$ or $LiPF_6$.

DSC measurements on deintercalated and fully intercalated CB and graphite electrodes were carried out using a Mettler DSC 30, TA 4000 system. The electrodes prepared for DSC measurements were charged and discharged in potentiostatic mode on a MacPileII™ system with steps of 10 mV and a current density cut-off limit of <0.01 mA/cm^2. The various components of the half-cells and combinations thereof were studied in the temperature range 30–300°C at a 5°C/min rate. The DSC samples were prepared by dismantling the cells in a glove-box and punching out standard discs, which were placed in Al crucibles. The current-collector was placed against the Al surface to ensure minimum contact between the walls of the crucible and the carbon samples. The same amount of current collector was used in the reference crucible. A typical sample weight was 3 mg.

2.3. High-potential region

The 3.0–5.5 V versus Li/Li^+ range is hereafter referred to as the high-potential region. Cyclic voltammetry was performed on a EG&G Princeton Instruments 783 potentiostat, using a scan rate of 60 mV/min. Cyclic voltammetry studies were made on CB electrodes containing the three different binders. To separate the reactions originating from the different components of the electrode, measurements were also made on the binders separately and on the graphitised Al current-collector as such, without any active material. Composite electrodes were cycled in two different electrolytes, using either $LiBF_4$ or $LiPF_6$. Potentiostatic and galvanostatic cycling were carried out on a MacPileII™ or Digatron BTS-600 potentiostat between 3.0 and 4.5 V. DSC measurements were carried out as above on $LiMn_2O_4$ electrodes cycled in this region and on the various components.

A Stoe & CIE GmbH STADI X-ray powder diffractometer (Cu $K\alpha_1$ radiation) with a position-sensitive detector, was used for ex situ XRD studies in transmission mode on charged CB electrodes to find evidence of any possible anion intercalation.

3. Results and discussion

3.1. Powder characterisation

The surface area of CB (80 m^2/g) was, as expected, substantially higher than that for graphite or $LiMn_2O_4$ (4.0 and 3.0 m^2/g, respectively). To probe the effect of ball-milling on surface area, the powders were ball-milled in cyclohexane (to simulate electrode manufacturing conditions) and then dried. The surface area remained almost the same for CB but, in the case of $LiMn_2O_4$, the surface area increased to 4.5 m^2/g. The surface area of ball-milled graphite was not measured but was not expected to increase dramatically.

Many different models have been proposed for the structure of CB [16]. In a microstructural model proposed by Riley, the carbon black particle can be depicted as a random distribution of small crystallites [17]. The diffraction pattern of Shewinigan black used in this study can be seen in Fig. 1. Scherrer's formula gave the size of mosaic blocks in the powder to be ca. 2 nm.

3.2. Low-potential region

Galvanostatic cycling of the electrodes consisting of 90 wt.% CB and 10 wt.% binder was performed in the low-potential region. Both EPDM and PVdF were used as binder, but no difference in the cycling performance of the electrodes could be discerned in terms of reversible and irreversible capacity. If not stated otherwise, EPDM is used hereafter. A high discharge capacity of 520 mAh/g was found during the first cycle, followed by a relatively constant capacity during the subsequent 10 cycles (Fig. 2). The cycling performance of Woxna graphite is included for comparison. The capacity for the 10th cycle is as high as 180 mAh/g, which shows that the CB is indeed an active component in the composite anode, and intercalates lithium reversibly. This would seem to be a normal value for carbon black materials; acetylene black, another commonly used CB material, has a reversible capacity of 190 mAh/g [8], also with a high first-cycle irreversible capacity.

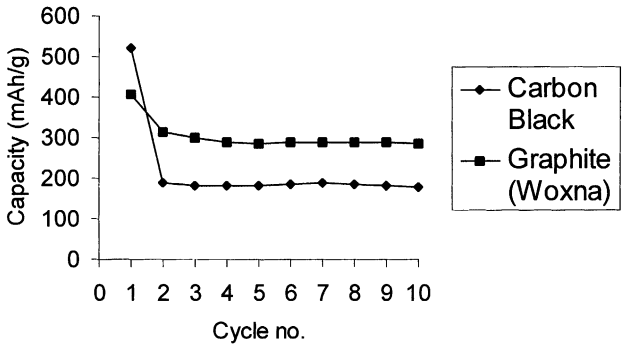

Fig. 2. Cycling performance of a 90 wt.% CB and 10 wt.% EPDM electrode in a 1 M $LiBF_4$ EC/DMC 2:1 electrolyte.

The first-cycle irreversible capacity was calculated for the different mixtures of CB and graphite (Fig. 3). It is defined here as the difference (in percent) between the charge consumed and the charge released during the first cycle. A clear correlation can be seen between irreversible capacity and CB content, with a substantial increase in irreversible capacity with increasing amount of CB. Earlier studies have shown that graphite electrodes with a large BET surface area exhibit a larger irreversible capacity than electrodes with a smaller surface area [18–19]. We, therefore, expect an increase in irreversible capacity on adding more of the high surface area CB. Xing and Dahn showed that the irreversible capacity is not only a measure of the amount of SEI, but can also relate to the reduction of surface species on the carbon [20]. Many chemically active groups are likely to be present on the high surface area CB, and the reduction of these during the first cycle will contribute to the

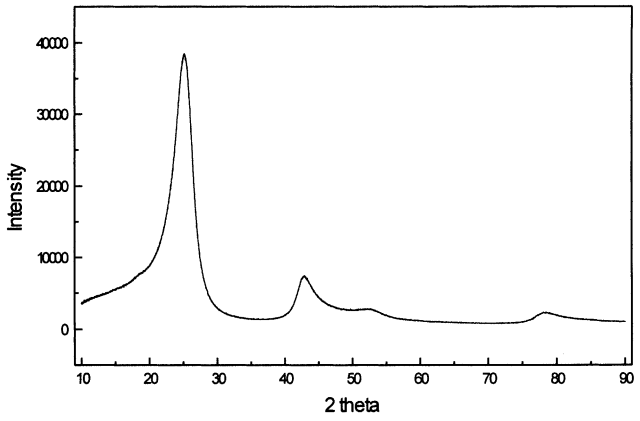

Fig. 1. X-ray diffractogram of Shewinigan black.

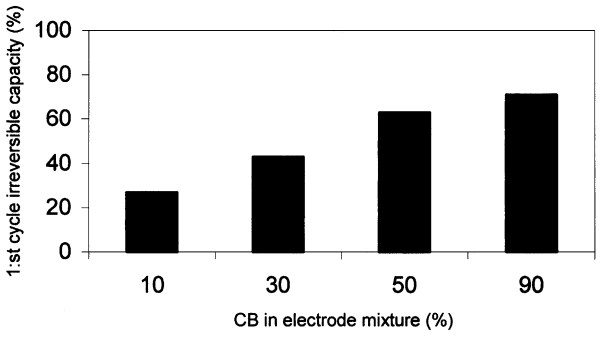

Fig. 3. First-cycle irreversible capacity for anodes made from Woxna graphite and increasing amounts of CB.

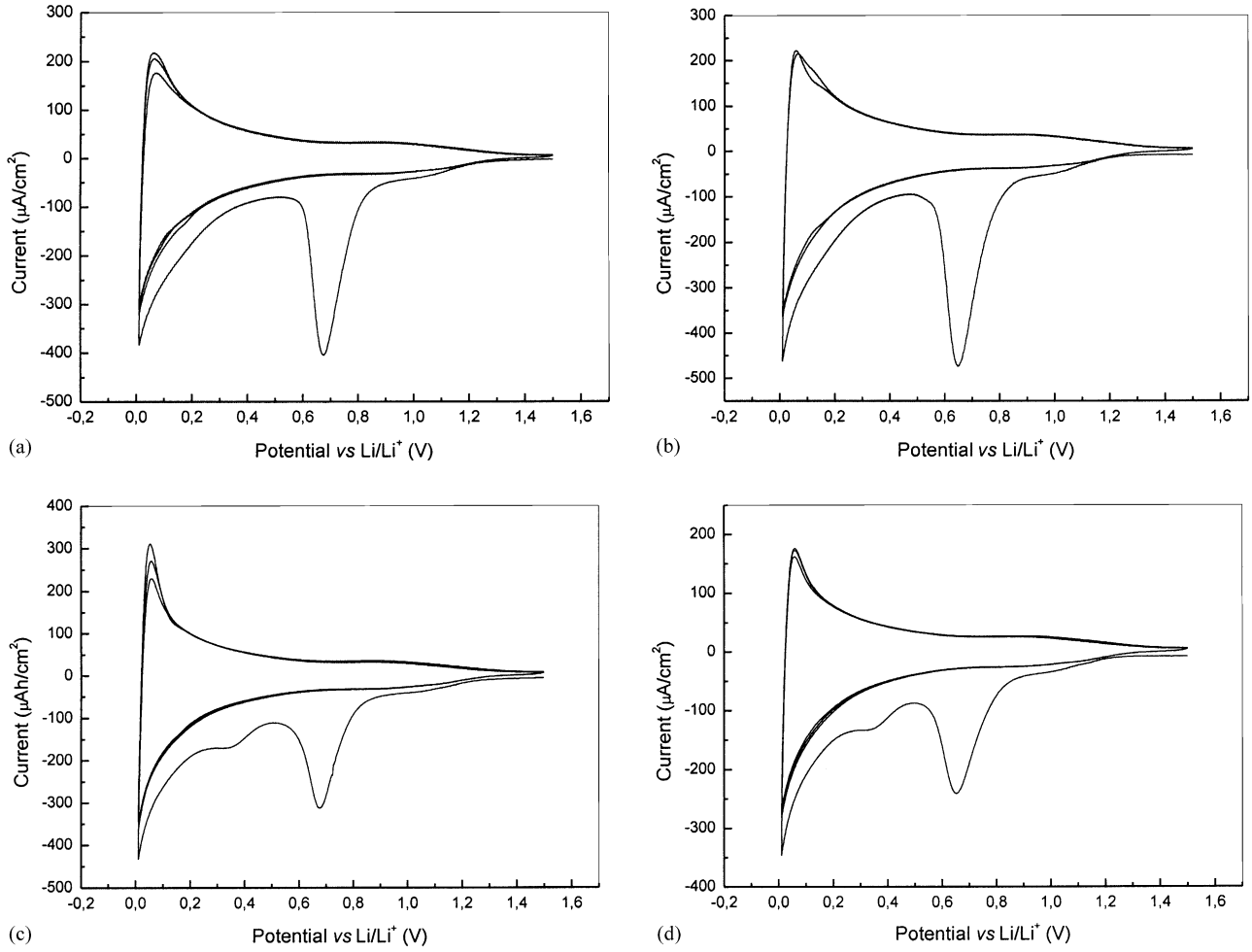

Fig. 4. Cyclic voltammograms of CB electrodes measured at a scan rate of 10 mV/min; 90 wt.% CB was used with 10 wt.% of the binder indicated and two different electrolytes consisting of EC/DMC 2:1 and 1 M of the salt stated: (a) EPDM + $LiPF_6$; (b) EPDM + $LiBF_4$; (c) PVdF + $LiBF_4$; and (d) PVdF + $LiPF_6$.

first-cycle irreversible capacity under SEI formation. Moreover, since this is believed to occur mainly on the edge-planes [21], and CB is highly disordered with effectively a high density of edge-planes, considerable SEI formation can be expected. Reducing the CB content in the composite anode will thus be crucial to minimising the first-cycle capacity loss.

A strong peak around 0.65 V can be seen in the cyclic voltammograms for the low-potential region, during the first cycle, for all combinations of electrolyte and binder when cycling 90 wt.% CB and 10 wt.% binder against lithium (Fig. 4a–d). This peak disappears in the subsequent cycles and can be attributed to the formation of an SEI-layer on the CB electrode. The next cycles show reversible lithium intercalation/deintercalation. A clear difference can be seen, however, between using EPDM and PVdF as a binder. In the PVdF case, an extra peak is observed at 0.35 V in the first cycle for both electrolytes. This could be due to some additional reduction processes involving the fluorinated binder at this potential.

3.3. High-potential region

As presented by many researchers earlier, the spinel $LiMn_2O_4$ material is a good Li-insertion material in the 3.5–4.3 V region [1,2], and our measurements also show good capacities in this region. But as today's Li-ion batteries move towards cathode materials operating in the 5 V region [15] we extended this study above the conventional potential cut-off limit in order to search for side-reactions. Cyclic voltammetry shows that a $LiMn_2O_4$/CB/EPDM 80:15:5 by weight composite electrode cycles well in the 3.4–5.0 V region in an 1 M $LiBF_4$ EC/DMC 2:1 by volume electrolyte (Fig. 5a). The result is quite different, however, for $LiPF_6$ salt in the same solvents. A large irreversible oxidation peak is seen at 4.6 V, and no reversible capacity is obtained in the subsequent cycles (Fig. 5b). None of the samples cycle after one oxidation, regardless of the electrolyte used, on extending the voltage range from 3.4 to 5.5 V. Above 5.0 V, the $LiBF_4$ electrolyte is easily oxidised, and the oxidation products precipitate onto the electrode surfaces; this may

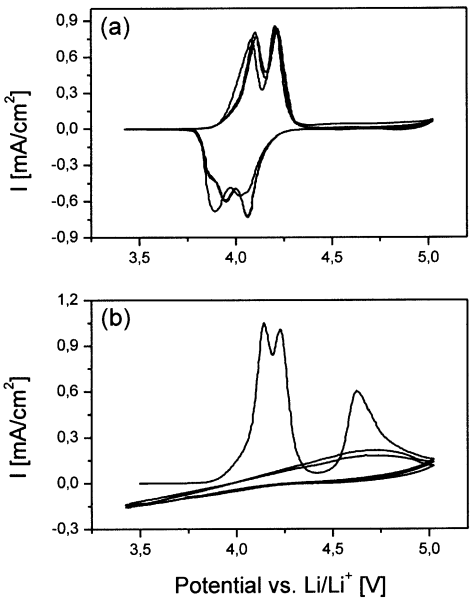

Fig. 5. Cyclic voltammograms of $LiMn_2O_4$ electrodes measured at a scan rate of 60 mV/min; 80 wt.% $LiMn_2O_4$, 15 wt.% CB and 5 wt.% of EPDM was used in two different electrolytes consisting of EC/DMC 2:1 and 1 M of the salt stated: (a) $LiBF_4$; (b) $LiPF_6$.

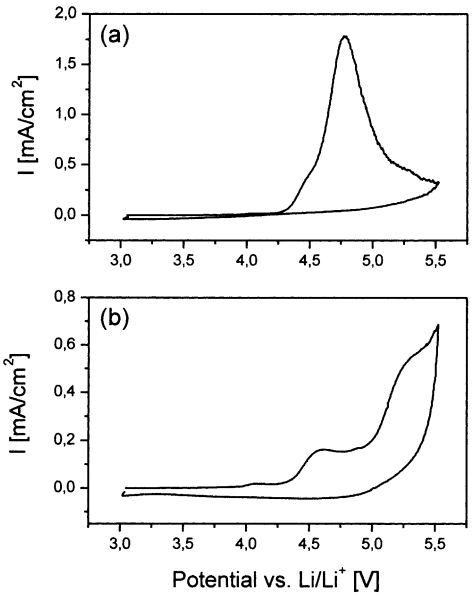

Fig. 6. Cyclic voltammograms of CB electrodes measured at a scan rate of 60 mV/min; 90 wt.% CB was used with 10 wt.% of EPDM in two different electrolytes consisting of EC/DMC 2:1 and 1 M of the salt stated: (a) $LiPF_6$; (b) $LiBF_4$.

lead to a higher cell impedance and loss of reversible capacity.

To gain a better insight into the effect of CB and binder on the performance of Li-ion cathodes, we have constructed electrodes containing no active $LiMn_2O_4$ material, only CB and binder. We have used three different binders: EPDM, Kraton G and PVdF. EPDM is a saturated amorphous elastomer with a glass-transition at ca. −50°C, based on a random copolymer of ethylene and propylene with ethyliden norbornen as cross-linker. Saturated elastomers are very resistant to oxygen and water. Kraton G is a thermoplastic elastomer, here comprising a starblock-copolymer where the arms are polyisoprene and poly((ethene-co-butene)-block-styrene), giving it more adhesive properties. Both EPDM and Kraton G are non-fluorinated and structurally more complex than PVdF, which comprises –(CH_2–CF_2)– blocks.

Electrodes with CB/EPDM 90:10 by weight were cycled over the same potential range as the $LiMn_2O_4$ composite electrode cells. Oxidation peaks at 4.5 V and 4.8 V are clearly seen for the $LiPF_6$ electrolyte (Fig. 6a). The same peaks are seen for $LiBF_4$, but the 4.8 V peak is 10 times smaller (Fig. 6b). The various reaction potentials are summarised in Table 1. Oxidation peaks for electrodes with CB/Kraton G 90:10 by weight appear in the same potential region as for EPDM (Fig. 7). This implies that these reactions are not necessarily dependent on binder-type, but are common to all the non-fluorinated binders. The high potential measurements on PVdF together with CB show no large reactions before ca. 5.0 V, where the electrolytes begin to oxidise (Fig. 8). The peaks at 4.5–4.8 V must, therefore, derive from reactions involving the non-fluorinated binders. Although water oxidation occurs in approximately the same

Table 1
A summary of the oxidation reaction potentials observed in cyclic voltammetry studies made at 1 mV/s for different electrode/binder combinations in an EC/DMC 2:1 electrolyte using 1 M $LiPF_6$ or $LiBF_4$ salt

Electrode	Weight ratio	$LiPF_6$ salt (V)	$LiBF_4$ salt (V)
$LiMn_2O_4$/CB/EPDM	80:15:5	4.62	4.58, 4.88, 5.24
CB/EPDM	90:10	4.53, 4.77	4.59, 4.89, 5.32
CB/PVdF	90:10	5.32	5.32
CB/Kraton G	90:10	4.45, 4.70	
EPDM	100	4.50	4.41, 5.17
Graphitised Al	100	4.96, 5.27	

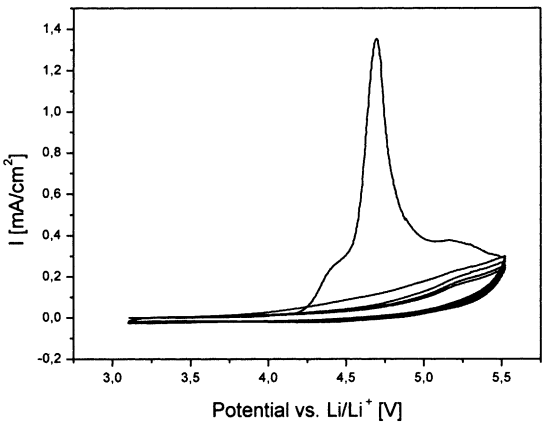

Fig. 7. Cyclic voltammogram of a CB electrode, measured at a scan rate of 60 mV/min; 90 wt.% CB was used with 10 wt.% of Kraton G in EC/DMC 2:1 with 1 M $LiPF_6$ electrolyte.

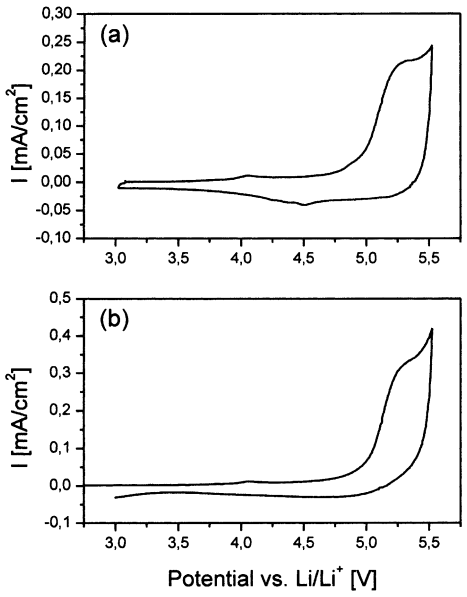

Fig. 8. Cyclic voltammograms of CB electrodes measured at a scan rate of 60 mV/min; 90 wt.% CB was used with 10 wt.% of PVdF in two different electrolytes consisting of EC/DMC 2:1 and 1 M of the salt stated: (a) $LiPF_6$; (b) $LiBF_4$.

potential range, it is unlikely that water is the source of these reactions since they are only observed for non-fluorinated binders, and the amount of water in the electrolytes were determined to <20 ppm by Carl Fischer titration.

Anion intercalation has been reported for graphite electrodes in the high potential range [22–23]. It was not possible to use in situ XRD on "coffee-bag" type cells with CB/EPDM 90:10 electrodes due to the low intensity of the CB peaks which intend to drown in the background from the other materials. Instead, ex situ XRD measurements were made in an inert atmosphere on cycled samples to achieve better resolution. No shifts were seen in the CB peaks after cycling, from which we conclude that no anion intercalation had occurred.

The DSC plot in Fig. 9 shows the melting of EC/DMC around 20°C, and another two-step endothermic electrolyte reaction at 200–300°C. We would expect a surface film to react upon heating in a similar way as we have observed with the composite $LiMn_2O_4$ electrodes [24] and the low potential samples in this study. No peaks beside those from the electrolyte residues could be found for the used CB-electrode samples, thus implying that the reactions indicated in the CV do not correspond to the formation of a surface film from electrolyte decomposition products.

Pure EPDM on Al-foil gives CV peaks at the same positions as for the CB composite electrodes, but with a much lower current response, despite loading for the EPDM film being 10 times greater than in the composite electrodes (Fig. 10). No DSC response from anything but the electrolyte could be detected here either. The addition of CB to the electrode clearly enhances the reactions around 4.5–4.8 V.

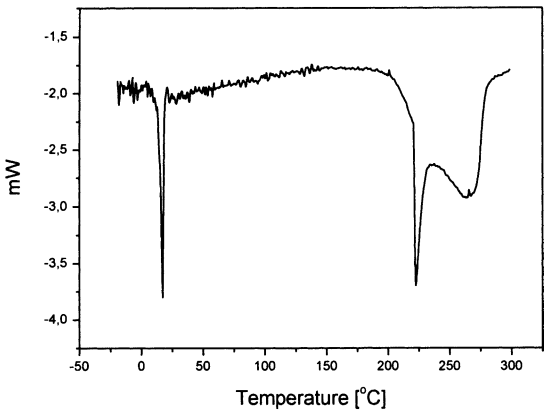

Fig. 9. DSC measurement at 5°C/min of a CB electrode that has been cycled one sweep at a scan rate of 60 mV/min; 90 wt.% CB was used with 10 wt.% of EPDM in EC/DMC 2:1 with 1 M $LiPF_6$ electrolyte.

A possible explanation to the CV peaks in the CB/non-fluorinated binder electrodes could be that some reaction occurs between the binder and acidic components in the electrolyte. This would also explain why the current response is larger for $LiPF_6$ than $LiBF_4$; $LiPF_6$ is known to be more sensitive to impurities in the solvents and breaks down more easily to form acidic side-products (reactions 1 and 2), while $LiBF_4$ is more stable [25]:

$$LiPF_6(sol.) \leftrightarrow LiF(s) + PF_5(g) \quad (1)$$

$$PF_5(g) + H_2O \rightarrow 2HF + PF_3O(s) \quad (2)$$

Results from the experiments with pure binder indicates that what we detect is a surface reaction and it is strongly increased by adding CB to the electrode. The large surface

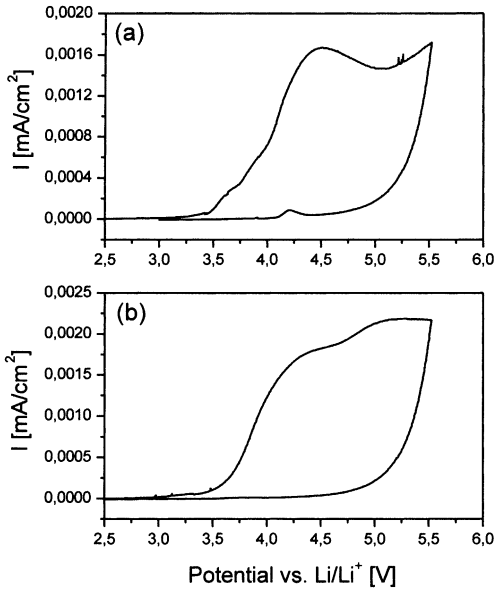

Fig. 10. Cyclic voltammogram of an EPDM film on Al, measured at a scan rate of 60 mV/min, in an electrolyte consisting of EC/DMC 2:1 with 1 M salt: (a) $LiPF_6$; (b) $LiBF_4$.

area of CB results in a larger contact surface between electrolyte and binder, and thereby enhances any reactions between them.

An alternative explanation could be that unreacted monomers in the binder react in the 4.5–4.8 V potential region. The binder could cross-link, with the anions as initiators, to form a stiffer framework; this would lead to the cell failure seen in Fig. 5b after the initial charge. Both PF_6^- and BF_4^- can initiate electropolymerisation in the presence of traces of protic substances, so this does not explain why there should be a larger current for the PF_6^- anion, unless it is a more efficient initiator than BF_4^- [26,27]. We can note that only a small fraction of the EPDM is the cross-linking polymer, and yet the oxidation current from the reaction is quite large.

Graphitised Al used as current collector gives much better adhesion properties for the composite cathode. We have observed strange oxidation-peaks using these current collectors, and have, therefore, tested the modified current collectors separately in cells (Fig. 11). A nucleation process can be occurring during the first oxidation sweep, which causes the subsequent reduction processes during the first reduction sweep. The reduction products are then oxidised in the second oxidation sweep. Thereafter, the reactions level out as there are no more species that can react, and the reactions are clearly irreversible.

3.4. DSC measurements/low-potential region

DSC measurements were performed on fully intercalated and deintercalated CB and on graphite electrodes in the low-potential region. A typical DSC trace of a fully intercalated CB electrode in a 1 M $LiBF_4$ EC/DMC 2:1 electrolyte can be seen in Fig. 12a, where the exothermic reaction in the temperature range 60–140°C is due both to reactions of the SEI-layer and to lithium depletion of the carbon. For a deintercalated sample, the exothermal peak in the 60–140°C range is much smaller and due only to decomposition of the SEI-layer (Fig. 12b). The behaviour is similar for the fully intercalated graphite electrode as seen in Fig. 12c. The CB particle size is much smaller than for graphite and the distribution is narrower, which can explain the sharper exothermal peak in the CB case. The endothermic reaction at ~200–250°C can be attributed to solvent/salt decomposition, which would correspond well to similar studies on composite graphite anodes [9], where the peak in the 60–140°C range was found to consist of two overlapping peaks; the size of the second peak could be correlated to lithium content. Two peaks could not be resolved here.

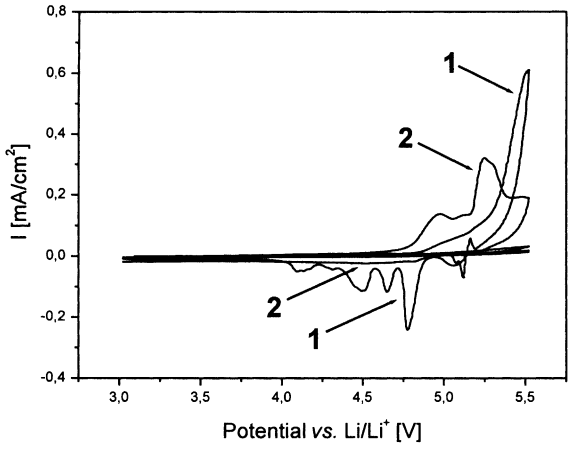

Fig. 11. Cyclic voltammogram of graphitised Al, measured at a scan rate of 60 mV/min, in EC/DMC 2:1 with 1 M $LiPF_6$ electrolyte. Oxidation and reduction sweeps 1 and 2 are indicated by the arrows.

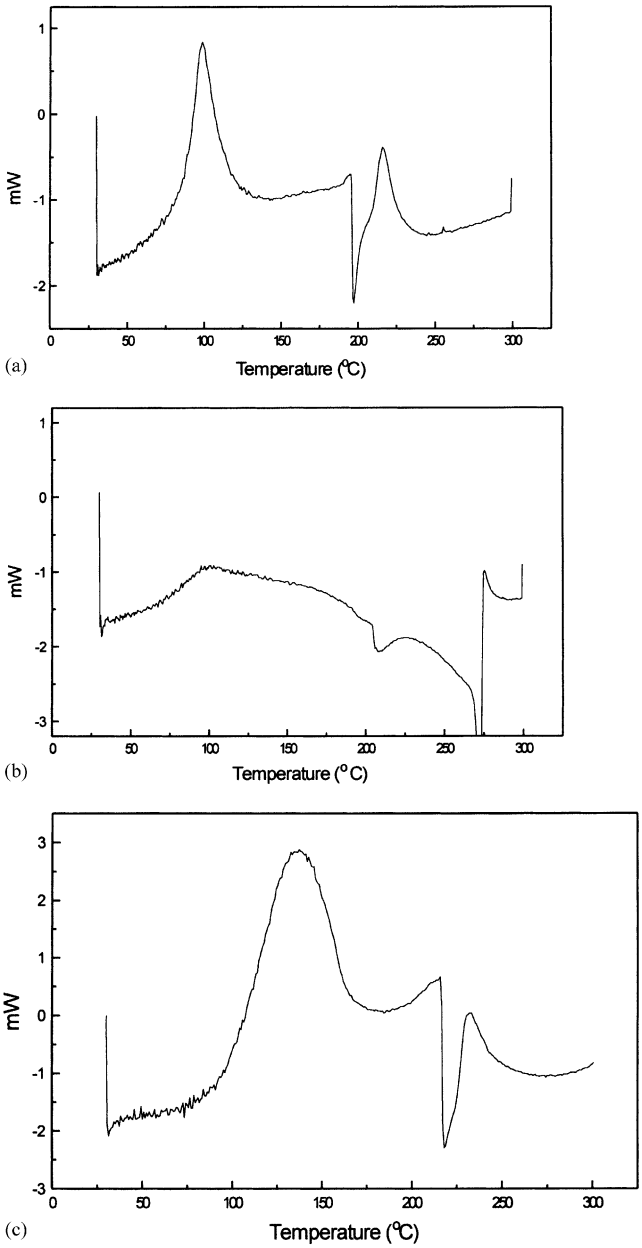

Fig. 12. DSC traces of CB electrodes with 10 wt.% EPDM binder in a 1 M $LiBF_4$ EC/DMC 2:1 electrolyte: (a) fully intercalated; (b) deintercalated; (c) a DSC trace of a fully intercalated graphite electrode in the same electrolyte.

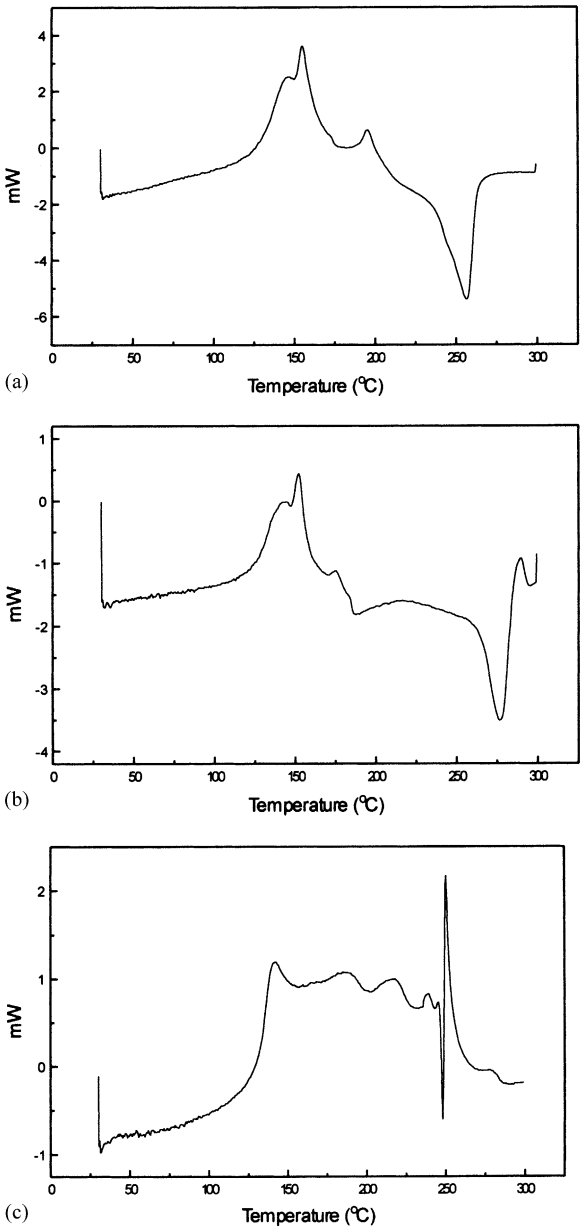

Fig. 13. DSC traces of CB electrodes with 10 wt.% EPDM binder in a 1 M $LiPF_6$ EC/DMC 2:1 electrolyte: (a) fully intercalated; (b) deintercalated; (c) a DSC trace of a fully intercalated graphite electrode in the same electrolyte.

A DSC trace from a fully intercalated CB electrode in a 1 M $LiPF_6$ EC/DMC 2:1 electrolyte is shown in Fig. 13a. The onset temperature for the SEI-layer reaction and lithium depletion is higher (~110°C) and the reactions continue up to ~180°C. In this region, two overlapping peaks can clearly be seen in the case of both intercalated and deintercalated electrodes (Fig. 13a and b). A fully intercalated graphite electrode in the same electrolyte is shown in Fig. 13c. The shape of the peaks is also quite different from the $LiBF_4$ case here as well. Earlier studies on graphite have attributed the first peak to SEI-layer decomposition and then a baseline shift due to CO_2 evolution [10]. Reactions between the lithiated electrode and the electrolyte were then found at around 200°C. Our results show a similar behaviour where, for a deintercalated sample, only the first peak remains at ~140°C. This peak is hence due to SEI-layer decomposition. ARC studies on lithiated carbon samples in an $LiPF_6$-based electrolyte have shown that a two-step process occurs on heating [11]. The first reaction is that of metastable (e.g. lithium-alkyl carbonates and semicarbonates) components of the SEI-layer decomposing into more stable (inorganic) compounds, and the second is from intercalated lithium reacting with the electrolyte (lithium depletion).

The heat of reaction was calculated from the exothermic peak for both intercalated and deintercalated CB electrodes in both electrolytes (Table 2). The difference in enthalpy between the intercalated and deintercalated samples is due to reactions involving expelled lithium depletion, and hence, corresponds to the lithium content in the samples. It is virtually the same for both salts, while total reaction enthalpy is much higher for $LiPF_6$, indicating stronger reactions originating from decomposition of the SEI-layer. The enthalpy for a deintercalated KS6 graphite electrode consisting of 5 wt.% CB and 5 wt.% EPDM in both electrolytes is also given in Table 2. The enthalpy is larger for $LiPF_6$ than $LiBF_4$. The reactions associated with SEI-layer decomposition are much stronger for the CB electrodes than for the graphite electrodes for both salts, due to the larger surface area of the CB, and hence, the more extensive SEI-layer. A thorough study of graphite electrodes at elevated temperatures with electrolytes using these two salts can be found in [28].

The thermal behaviour of different binders has been examined by Richard and Dahn [29] using the ARC method. EPDM was found to be more thermally stable than PVdF. We have made DSC studies on both fully intercalated and deintercalated CB electrodes using both EPDM and PVdF as binder. No additional reactions seem to occur involving the PVdF binder in this temperature range compared to the corresponding measurements with an EPDM binder. The reactions associated with SEI-layer decomposition begin at a higher temperature for $LiPF_6$ than $LiBF_4$, irrespective of the type of binder used.

Table 2
Heat of reaction per mass electrode calculated for the first exothermal reaction for fully intercalated or deintercalated CB or graphite (KS6) electrodes (all EPDM-binder) in an EC/DMC 2:1 electrolyte with 1 M of the salt (given in brackets)

Sample	ΔH (J/g)
Fully intercalated ($LiBF_4$)	142
Deintercalated ($LiBF_4$)	73
Fully intercalated ($LiPF_6$)	220
Deintercalated ($LiPF_6$)	136
Deintercalated graphite ($LiBF_4$)	33
Deintercalated graphite ($LiPF_6$)	56

4. Conclusions

The complexity of the chemical and electrochemical reactions occurring in Li-ion batteries has been demonstrated here by showing the influence of each single component (and combinations of components) used in the system.

The CB shows a large irreversible capacity when cycled in the low-potential region; this has been quantified in this study. The thermal stability of the SEI-layer on a CB electrode was found to be similar to that formed on graphite. The onset temperature for degradation of this SEI-layer was higher for $LiPF_6$ than $LiBF_4$ salt for both CB and graphite electrodes. The reactions involving SEI-layer decomposition were, however, stronger for CB than for graphite. The thermal stability of anodes using both EPDM and PVdF was also probed.

In the high-potential region, large irreversible oxidation reactions were observed which clearly influence battery performance. These reactions could not be attributed to anion intercalation or to surface-film formation, but rather to reactions involving the binder and electrolyte salt; $LiPF_6$ was found to give stronger oxidation reactions than $LiBF_4$. Non-fluorinated binders were found to show clearly different reactions from the fluorinated binder.

Acknowledgements

This work has been supported by grants from The Foundation for Environmental Strategic Research (MISTRA), the EU (Joule III) Non-Nuclear Energy Sources Program, The Swedish Natural Science Research Council (NFR) and The Swedish Board for Technical Development (NUTEK). We would also like to thank Dr. Patric Jannasch for his helpful suggestions and supply of material (Kraton G).

References

[1] J.-M. Tarascon, F. Coowar, G. Amatucci, F.K. Shokoohi, D.G. Guyomard, J. Power Sources 54 (1995) 103.
[2] A. Blyr, C. Sigala, G. Amatucci, D. Guyomard, Y. Chabre, J.-M. Tarascon, J. Electrochem. Soc. 145 (1998) 194.
[3] P. Arora, R.E. White, M. Doyle, J. Electrochem. Soc. 145 (1998) 3647.
[4] G. Li, R. Xue, L. Chen, Y.Z. Huang, J. Power Sources 54 (1995) 271.
[5] K. Takei, N. Terada, K. Kumai, T. Iwahori, T. Uwai, T. Miura, J. Power Sources 55 (1995) 191.
[6] A.K. Sleigh, U. von Sacken, Solid State Ionics 57 (1992) 99.
[7] T.D. Tran, J.H. Feikert, X. Song, K. Kinoshita, J. Electrochem. Soc. 142 (1995) 3297.
[8] R. Yazami, M. Deschamps, J. Power Sources 54 (1995) 411.
[9] A.M. Andersson, K. Edström, J.O. Thomas, J. Power Sources 81/82 (1999) 8.
[10] A. Du Pasquier, F. Disma, T. Bowmer, A.S. Gozdz, G. Amatucci, J.-M. Tarascon, J. Electrochem. Soc. 145 (1998) 472.
[11] M.N. Richard, J.R. Dahn, J. Electrochem. Soc. 146 (1999) 2068.
[12] Z. Liu, A. Yu, J.Y. Lee, J. Power Sources 74 (1998) 228.
[13] D. Guyomard, J.-M. Tarascon, Solid State Ionics 69 (1994) 222.
[14] D.H. Jang, S.M. Oh, Electrochim. Acta 43 (1998) 1023.
[15] H. Kawai, M. Nagata, H. Kageyama, H. Tukamoto, A.R. West, Electrochim. Acta 45 (1999) 315.
[16] K. Kinoshita, Carbon, Wiley, New York, 1988.
[17] H.L. Riley, Chem. Ind. 58 (1939) 391.
[18] R. Fong, U. von Sacken, J.R. Dahn, J. Electrochem. Soc. 137 (1990) 2009.
[19] M. Winter, P. Novák, A. Monnier, J. Electrochem. Soc. 145 (1998) 428.
[20] W. Xing, J. R Dahn, J. Electrochem. Soc. 144 (1997) 1195.
[21] D. Bar-Tow, E. Peled, L. Burstein, J. Electrochem. Soc. 146 (1999) 824.
[22] R. Santhanam, M. Noel, J. Power Sources 66 (1997) 47.
[23] J.A. Seel, J.R. Dahn, J. Electrochem. Soc. 147 (2000) 892.
[24] T. Eriksson, A. Andersson, A. Bishop, T. Gustafsson, J.O. Thomas, in press.
[25] A. Du Pasquier, A. Blyr, P. Courjal, D. Larcher, G. Amatucci, B. Gérand, J.-M. Tarascon, J. Electrochem. Soc. 146 (1999) 428.
[26] G. Mengoli, G. Vidotto, J. Appl. Polym. Sci. 18 (1974) 3095.
[27] S. Nakahama, K. Hashimoto, N. Yamazaki, Polym. J. 4 (4) (1973) 437.
[28] A. M. Andersson, K. Edström, in press.
[29] M.N. Richard, J.R. Dahn, J. Power Sources 83 (1999) 71.